

## Positive transformations in intrinsic bioconstituents due to briquetting of soybean crop residues



Sandip Gangil \*

Agricultural Energy and Power Division, Central Institute of Agricultural Engineering, Bhopal 462038, MP, India

### ARTICLE INFO

#### Article history:

Received 9 February 2015

Accepted 8 May 2015

Available online xxxx

#### Keywords:

Thermogravimetry

Kinetics

Activation energy

Reactivity

Briquetted biofuel

Soybean crop residues

### ABSTRACT

Thermogravimetric spectra of binderless briquettes and its raw material, soybean crop residues, were critically analyzed to ascertain the changes occurring in the intrinsic biopolymeric components such as hemicellulose, cellulose and lignin due to briquetting stresses. Transitions of thermogravimetric signals and activation energy levels were analyzed and discussed. The distinct and sharp signals related to the secondary charring process at the high temperature regime in thermogravimetry were noticed in briquettes as compared to these signals in raw residue. Integral isoconversional Friedman kinetics treatment was used to compute the conversion fraction dependent activation energies. Deconvolution analysis of differential thermograms was done to diagnose the internal thermogravimetric transformations. It established the lesser reactivity and better consolidation in case of briquetted biofuel.

© 2015 International Energy Initiative. Published by Elsevier Inc. All rights reserved.

### Introduction

Conversion of crop residues (CR) to solid compact briquetted fuel (Gangil, 2014a,b, 2015a,b; Chen et al., 2009; Đerčan et al., 2012; Rajkumar and Venkatachalam, 2013; Singh et al., 2007, 2008) is one of the most promising management options to enhance the utility of CR for purpose of energy generation obtaining the energy sustainability in rural areas of developing countries. During briquetting, the stresses are applied on crop residues which change the internal matrix of biomaterial. The physico-chemical transformations occur due to briquetting stresses. In raw form, the handling and storage of CR are difficult during energy generation because of looseness of CR (Gangil, 2014a,b, 2015a, b; Tripathi et al., 1998; Tumuluru et al., 2010; Grover and Mishra, 1996; Purohit et al., 2006; Mythil and Venkatachalam, 2013). Also, CR does not flow properly in the reactors of bioenergy devices due to their irregular shape & size, and light weight. The crop residue based energy and power generation systems need better fuel flow in their bio-reactors which can be obtained using uniform size of biofuels. Uniformity in fuel shape and size avoids the choking and blockages of fuel in a reactor of bioenergy device. The CR can be used as substitute biofuel against wood chips in the biomass based power generation systems and combustion devices.

The briquettes can be produced from lignocellulosic crop residues (Gangil, 2014a,b, 2015a,b). The raw lignocellulosic material is powdered and fed in a pressing unit for briquetting. The lignocellulosic

materials can be briquetted without a binder as the lignin present in these materials can itself act as a binding agent. The briquetting systems available are screw-press type, piston-press (die-punch) type and rotary-die-roller type (Gangil, 2014a,b, 2015a; Tripathi et al., 1998; Tumuluru et al., 2010; Grover and Mishra, 1996). A pressing unit puts compressive stresses on the raw CR in confined and semi-confined environment. In piston-press type systems, the raw bio-material is compressed so that the raw biomaterial can be extruded during compaction through the die. Due to stresses the temperature of biomaterial raises which changes the mutual linkages of biocomponents to form the briquette. In a screw press type briquetting machine, a conveying screw continuously presses the biomaterial through a die. The energy consumed per unit output of briquetting is higher in the case of screw-press type systems as compared to piston press systems.

Major bioconstituents of lignocellulosic crop residues are cellulose, hemicellulose and lignin. During the briquetting, a high pressure is exerted on biomaterials, which raise the temperature of CR. Basically, under the process of briquetting, an intrinsic biopolymeric matrix is placed under the stresses. Therefore, the stresses bring the physico-chemical transformations in each of intrinsic biopolymer. Due to heating of biomaterials in briquetting, some amount of moisture in the loose CR evaporates. Due to densification, biopolymers like, hemicellulose, cellulose and lignin, also pass through positive changes to form the briquetted fuel. When biomaterial is stressed more than 100 MPa or higher raising the temperatures of biomaterial above 200 °C, the softening of lignin occurs, and soft lignin binds the particles of biomaterials, tightly and thus, lignin acts like a binding agent (Gangil, 2014a,b, 2015a,b; Tumuluru et al., 2010). All lignocellulosic crop residues are

\* Tel.: +91 755 2521132, +91 9754913685; fax: +91 755 2734016.

E-mail addresses: gangilsandip@yahoo.co.in, gangils@yahoo.com, gangil@ciae.res.in.

briquettable by choosing the appropriate levels of the process parameters of the briquetting (Fengmin and Mingquan, 2011; Kaliyan and Morey, 2009).

A reliable and in-depth study of internal physico-chemical transformations in intrinsic biopolymers of a biomaterial can be accomplished using the thermogravimetric analysis (TGA) in which the biomaterial is subjected to heat in a precisely monitored and controlled chamber (Slopiecka et al., 2012; Jeguirim et al., 2014). We can also understand the thermal degradation behavior and patterns of different biocomponents. Thermal degradation of biomaterial occurs broadly in four stages namely in the moisture release, the hemicellulose degradation, the cellulose degradation and the lignin degradation (Vasile et al., 2011). Thermal degradation of lignocellulosic biomaterials is basically addition of the independent degradations of their main components (Caballero et al., 1997). The devolatilization curve of bio-materials obtained in TGA is the sum of the contributions from individual intrinsic biocomponent (López-González et al., 2013). Degradation of each biocomponent could be assumed as a first order reaction considering the degradation of different intrinsic biocomponents as independent parallel reactions (Ledakowicz and Stolarek, 2002). The structure of hemicellulose is random, amorphous and weak, whereas the structure of cellulose is crystalline and strong (Sanchez-Silva et al., 2012). According to Sanchez-Silva et al. (2012), the lignin was the highest thermally stable component and this biopolymer showed thermogravimetric peaks in the wide range of temperatures (200–700 °C). Also, the peak related to lignin was found the flattest in DTG profile (Sanchez-Silva et al., 2012). Due to heavily cross-linked highly branched complex structure, degradation of lignin has been stated as very difficult (Gangil, 2014a,b, 2015a,b; Sanchez-Silva et al., 2012).

While comparing the thermal degradation of two biomaterials, the signals obtained during TGA may be critically studied. These signals give the information about ease and difficulty during the thermal degradation of specific biocomponents. Popular isoconversional treatments to execute the kinetics of thermal degradation are Friedman, Coats–Redfern, Kissinger–Akahira–Sunose (KAS), Ozawa–Fynn–Wall (Damartzis et al., 2011; White et al., 2011; Vyazovkin and Sbirrazzuoli, 2006; Janković, 2008; Wang et al., 2012; Sbirrazzuoli et al., 2009; Lu et al., 2009), etc. Friedman is a differential isoconversional treatment (Sbirrazzuoli et al., 2009), whereas Coats–Redfern, Kissinger–Akahira–Sunose (KAS) and Ozawa–Fynn–Wall are integral isoconversional treatments (Sbirrazzuoli et al., 2009). In all these methods, broadly four steps are used to calculate the activation energy. For example, in Friedman method, the first step is to find the Friedman curves. The second step is to extract the Friedman points (kinetics points) at selected isoconversional fractions. Third step is to draw the Friedman kinetics lines with higher coefficients of regression to obtain the slope of these lines. In the last step, the slopes of these kinetics lines are used to compute the activation energies which approximates to  $-E/R$ . The similar kinds of steps are conventionally used in the KAS and OFW methods. The major limitation of isoconversional methods is to obtain the high level of regression while fitting the linear equation in kinetics points which is not always possible in the practical situation while analyzing the lignocellulosic biomaterials. As the lignocelluloses have inter-linkages of different kinds of biopolymers, their degradation is a very complex process. Therefore, many a times, isoconversional treatments applied to thermogravimetric data do not yield adequate information while comparing more than one biomaterial. In such cases, a critical investigation of specific biopolymeric TG-signals is needed which can be done by deconvolution analysis. In deconvolution analysis, the DTG is divided in different peaks and the variations of these deconvoluted TG-signals are analyzed.

The present article is a first attempt to apply the deconvolution analysis on the soybean crop residues to study the effects of briquetting stresses. The soybean crop residues and the briquettes made from it were critically analyzed to see the physico-chemical transformations responsible for thermal stability in the case of a briquetted biofuel.

## Materials and methods

Soybean crop residues (SS) were gathered from farmer fields. Thermogravimetric analyses (TGA) of powdered SS and its briquettes (SB) were conducted to understand the variations in the internal configuration on the basis of the thermogravimetric signals using a thermogravimetric analyzer (model: pyris-6; by: Perkin Elmer). Thermogravimetry provided the data about the weight loss (%) of bio-material versus temperature or time (thermogram) during the thermal degradation process. Differential thermogram (DTG) was the first order derivative of thermogram that gave information with respect to weight loss rate versus temperature or time, i.e., showing the degradation rate profile (degradation rate,  $\% \cdot \text{min}^{-1}$ ). The location (temperature or time values) and amplitude ( $d\alpha/dt$  in DTG) of TG-signals are two available parameters that could be compared to diagnose the thermal hardening or softening of a particular component in two kinds of biomaterials under evaluation. Higher amplitude of TG-signals indicated towards the thermal loosening or vice versa. The amplitude was more closely related to the bond energies of molecules of a particular biocompound with other biocompound molecules. The amplitude of the TG-signal is linked with the adhesion of one kind of biocompound with other types. Activation energy can be considered as a combined effect of energy related to the bonds within one kind of biocompound, and the bonds of that particular biocompound with other kinds of biocompounds. Higher activation energy showed the higher thermal stableness or vice versa. Vamvuka et al. (2003) expressed that the peak height was directly proportional to the reactivity. The amplitude was taken as the major consideration in present article.

The recommended sowing period of the soybean crop (*Glycine max* (L.) Merr.) (Mandal et al., 2002; Nevase et al., 2012; Nevase et al., 2013), an important crop in central region (Madhya Pradesh) of the India, was in the last week of June and the crop length is 95–105 days. Normally, combine harvesters were used for harvesting, which left the threshed residues in the field, itself. After harvesting from these machines, the residues (soybean straw (SS)) were taken within one week of the harvesting from the farmers' field. The material brought from the farmers' field was powdered using a hammer mill. In making the briquettes, the powdered SS was pressed in a commercial piston-press briquetting system (rated power 35 kW; rated capacity 500 kg/h). The briquetting plant, shown in earlier writings (Dubey et al., 2009; Gangil, 2015a), is installed at Agricultural Energy and Power Division, Central Institute of Agricultural Engineering, Bhopal, India. The samples of raw powdered SS used for TGA had the particle size distribution values of >0.2 mm (14–16%), 0.2–0.4 mm (15–16%), 0.4–0.7 (37–39%), 0.70–1.4 mm (15–17%), 1.4–1.7 mm (13–15%) and <1.7 mm (0–2%). The temperature during the briquetting at the die-region of briquetting plant reached >200 °C. Gangil (2015a) has highlighted the characteristics of the raw and briquetted material.

In TG analysis, exactly the same thermogravimetric heating method was used for SS and SB. The heating method was to maintain the temperature at 35 °C in TGA for 2 min and then to raise the TGA-temperature at different heating rates ( $\beta$ ) from 35 °C to 1000 °C in nitrogen environment. For TGA experiments, four  $\beta$  (10, 20, 30 and 40 °C/min) were used.

### Kinetics using the integral isoconversional Friedman method

The Friedman kinetics equation (Sbirrazzuoli et al., 2009) is stated as

$$\ln\left(\frac{d\alpha}{dt}\right) = \ln(A) + \ln(f(\alpha)) - \frac{E}{RT} \quad (1)$$

$$\alpha = \frac{w_i - w_t}{w_i - w_f} \quad (2)$$

where;  $\alpha$ , conversion fraction;  $t$ , reaction time;  $A$ , Arrhenius pre-exponential factor;  $f(\alpha)$ , reaction model;  $E$ , activation energy;  $R$ ,

universal gas constant;  $T$ , reaction temperature (absolute); and the  $w_i$ ,  $w_t$  and  $w_f$  are the masses of biomaterial at initial, instantaneous and final stages of decomposition, respectively;

In isoconversional method the terms  $\ln(f(\alpha))$  and  $\ln A$  were assumed as constants at a specific value of  $\alpha$ . Thus, Eq. (1) took a form of linear equation with its slope equal to  $-E/R$ . The steps to compute the activation energies are given earlier in this writing.

## Results and discussion

### Beneficial transitions of TG-signals due to briquetting of raw soybean crop residues

First order derivatives of both bio-material (raw soybean crop residues and its briquette) obtained at four experimented heating rate were compared to diagnose the positive and negative variations in different thermogravimetric signals due to a briquetting process. Fig. 1 shows DTG plots with respect to temperature and conversion fraction of both biomaterials covering the region of dehydration. Fig. 2 shows the degradation of cellulosic and hemicellulosic biopolymers during pyrolytic thermal degradation. Fig. 3 is exploded view of DTGs of both biomaterials highlighting the lignin and secondary charring regions. In secondary charring region the gaseous ( $H_2$  or  $CH_4$  or both) evolution release occurred. In all figures, the degradation rates are negative as mass was reduced during the thermogravimetry.

The moisture evaporation lasted until 170 °C for SS and until 160 °C in SB, considering the effect of all experimented  $\beta$  (Fig. 1). The moisture TG-signals shifted towards a higher temperature with an increase in  $\beta$  for SS and SB. In comparison, moisture-signals were found at higher temperatures in SB as compared to SS at each  $\beta$  showing thermal stability of moisture in SB. The SS had relatively loose bound moisture. Some portion of moisture, present in SS, was evaporated during briquetting due to high temperature and the remaining moisture in briquettes

existed as internally bound moisture. The degradation rates (the amplitude of the TG-signal) related to moisture, were also low in SB as compared to SS at all  $\beta$ .

Broadly, the  $\alpha$ -zones for SS were obtained as 0–0.12, 0.10–0.21, 0.20–0.70, 0.65–0.85 and 0.83–0.97 related to moisture, hemicellulose, cellulose, lignin and secondary charring, respectively. In the case of SB, the moisture, hemicellulose, cellulose, lignin and secondary charring regions were in  $\alpha$ -range of 0–0.11, 0.12–0.18, 0.17–0.75, 0.75–0.90 and 0.89–0.95, respectively. Moisture existed below  $\alpha$ -value of <0.11 in the case of briquette and <0.12 in SS. Viewing the  $\alpha$ -dependent moisture TG-signals, it can again be concluded that the moisture in SB was more stable.

SB did not show distinct TG-signals of hemicellulose (Gangil, 2014a, b, c, d, e, 2015a, b; Chen and Kuo, 2011; Burhenne et al., 2013) during T-domain analysis (Fig. 2). However, a minor but noticeable lump related to hemicellulose in SB was experienced at  $\beta$  of 40 °C/min at temperatures near 250 °C. Dull lumps were seen at  $\alpha$ -value of 0.15, 0.14 and 0.16 at 10, 20, and 40 °C/min. Hemicellulose in the SS was noticed from 250 to 270 °C and found to shift towards higher temperature at higher  $\beta$  (Fig. 2). In hemicellulose region, the degradation rates in SS fell above the degradation rates in SB at each  $\beta$ . It showed that hemicellulose was thermally strong in SB. The position of the hemicellulose TG-signal was at higher temperatures in SS as compared to their position in the case of SB at 40 °C/min indicating the thermal softening of the hemicellulose in SB. Overall, It was concluded that hemicellulose related TG-signal almost subsided in SB which was one of the positive variations during the formation of the briquette from SS.

Cellulose (Gangil, 2014a, b, c, d, e, 2015a, b; Chen and Kuo, 2011; Burhenne et al., 2013) related lumps for SS and SB were noticed in the range of 300–370 °C and 300–380 °C, respectively (Fig. 2). These were found to shift towards higher temperature at higher  $\beta$  (Fig. 2) for both bio-materials. Cellulose degradation rates in SB were higher than the degradation rates in SS at  $\beta$ -values of 20 and 30 °C/min. At 10 and

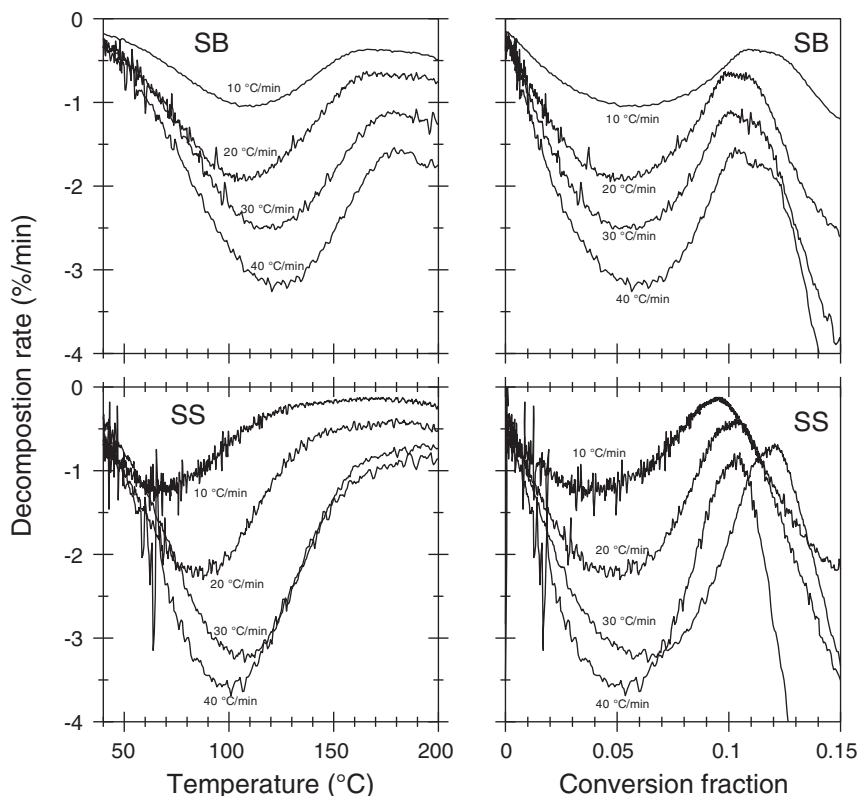


Fig. 1. DTG of SS and SB at different heating rates in T-domain and  $\alpha$ -domain for the dehydration region.

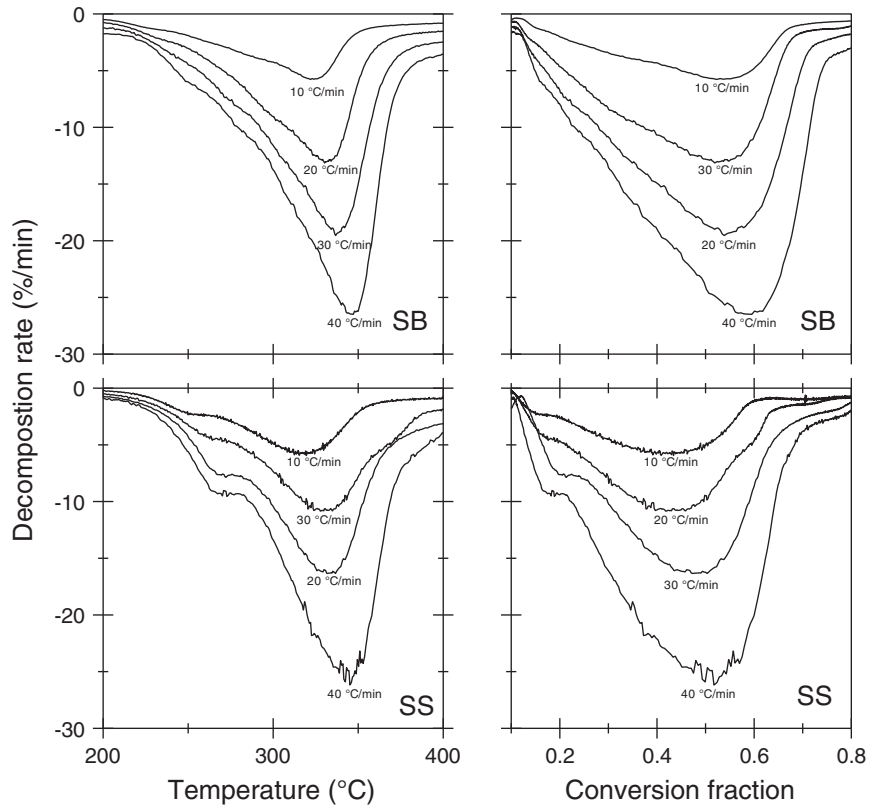


Fig. 2. Region of hemicellulose and cellulose degradation for SS and SB at different heating rates in T-domain and  $\alpha$ -domain.

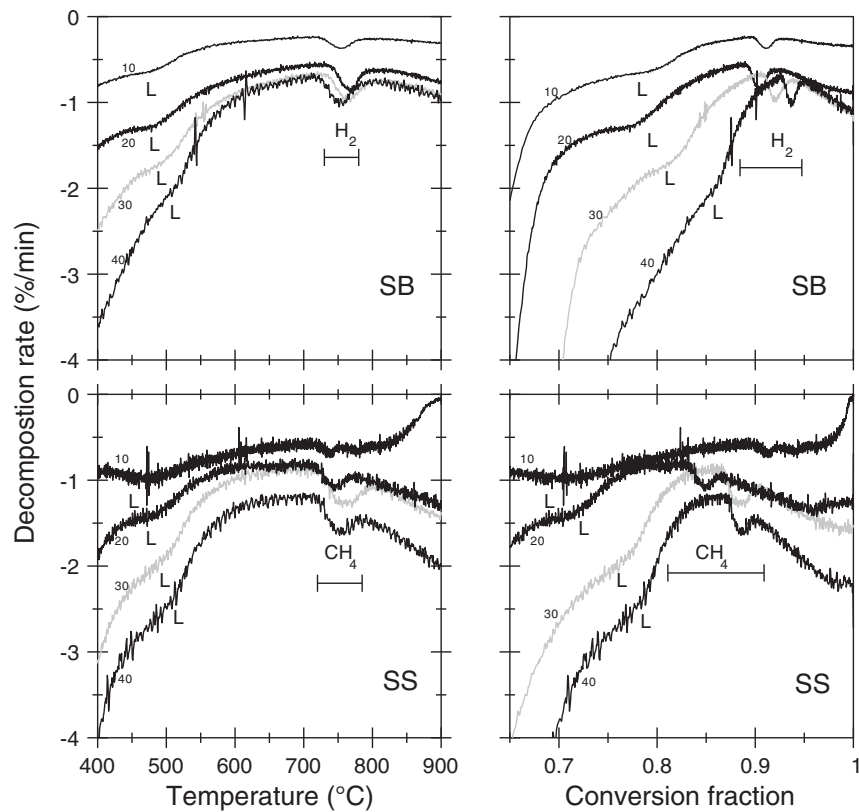


Fig. 3. Lignin and secondary charring region DTG-SS and DTG-SB in T-domain and  $\alpha$ -domain (the numbers 10, 20, 30, and 40 given near the curve, are the heating rates at which the particular DTG was taken).

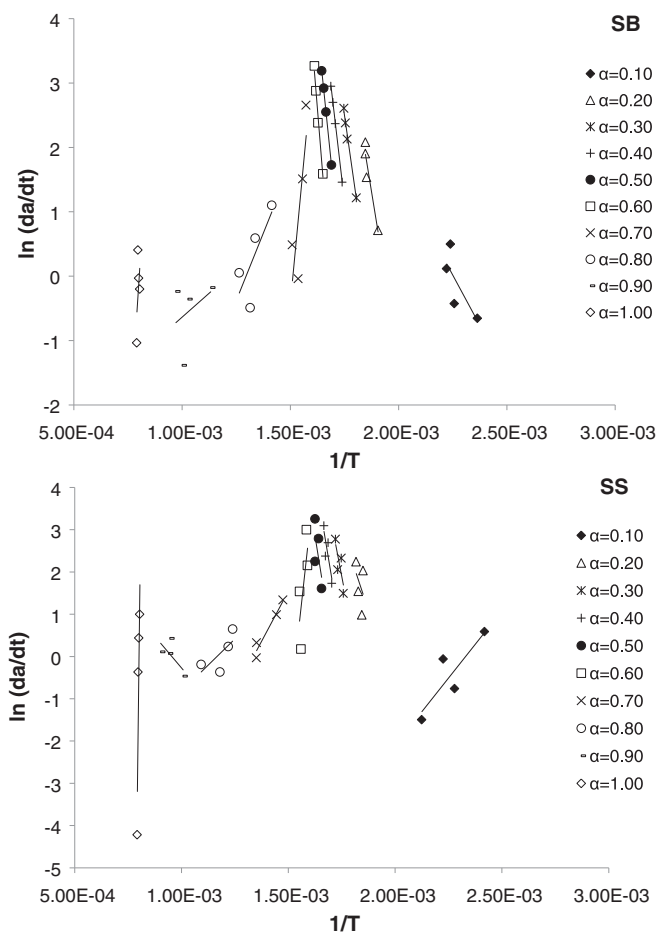


Fig. 4. Friedman Kinetics lines for SS and SB.

40 °C/min, the SB and SS showed similar amplitude of cellulose related TG-signals.

The hemicellulose degradation rates were lower as compared to the cellulose in SB and SS. According to López-González et al. (2013), during cellulose degradation region, a complex set of reactions as denitration, deacetylation and scission of O–N, C–O, C–C and C–H bonds might occur.

Weak lignin TG-signals (Gangil, 2014a,b,d,e, 2015a,b; Chen and Kuo, 2011; Burhenne et al., 2013; Faravelli et al., 2010) were seen near 500 °C (Fig. 3) in both the bio-materials. The lignin peaks were more flat and dull in SB whereas these were somewhat more pronounced in SS. The amplitudes of lignin degradation were higher in SS than in SB at all  $\beta$  showing that the lignin was relatively soft in SS.

Minor peaks were seen near 750 °C (Fig. 3) ascribed to gaseous evolution ( $\text{CH}_4$  or  $\text{H}_2$  or both) during a secondary charring process at the final stage of thermal degradation. The present article considered that gaseous evolution was due to changes in configurations of hemicellulose and lignin during briquetting, because in the present diagnosis, the hemicellulose TG-signals almost vanished and lignin TG-signals subsided in SB. However, Abdullah et al. (2010) mentioned that these types of gas evolution signals may be due to the degradation of lignin (Abdullah et al., 2010). Idris et al. (2010) noticed peaks in thermogravimetry of lignocellulosic bio-material (Palm Kernel Shell) in a temperature range of 650–750 °C (Idris et al., 2010). The release of methane and hydrogen was ascribed to these signals by them. They claimed that these peaks emerged due to the charring process. Therefore, TG-signals falling above 600 °C (located in 700–750 °C) can reasonably be ascribed to release of  $\text{CH}_4$  and  $\text{H}_2$ . The temperatures near  $720 \pm 10$  °C and  $750 \pm 20$  °C were related to the release of  $\text{CH}_4$  and  $\text{H}_2$ , respectively (Gangil, 2014a,b, 2015a,b; Idris et al., 2010).

The gaseous evolution ( $\text{CH}_4$  or  $\text{H}_2$  or both) peak in SB centered at  $\alpha$ -values of 0.91, 0.90, 0.92 and 0.94 at  $\beta$ -values of 10, 20, 30 and 40 °C/min, respectively. At 10 °C/min, the SS showed two peaks centering at  $\alpha = 0.91$  and  $\alpha = 0.94$ . These two signals were merged at higher heating rates and the single signal existing at a lower  $\alpha$ -value could sustain. SS related gaseous evolution ( $\text{CH}_4$ ) TG-signals were at  $\alpha$ -values of

Table 1

Linear correlation equations for Friedman isoconversional kinetic lines ( $\ln(d\alpha/dt)$  versus  $1/T$ ) for SS and SB.

$\alpha$	Soybean crop residue (SS)		Briquette (SB)	
	Equation of linear fitting for Friedman points	$R^2$	Equation of linear fitting for Friedman points	$R^2$
0.01	$y = -2396.2x + 7.4186$	0.4451	$y = -6174.7x + 18.205$	0.0426
0.05	$y = -5629.7x + 16.402$	0.9885	$y = -11225x + 30.045$	0.771
0.10	$y = 6378.1x - 14.859$	0.7549	$y = -6257.3x + 14.094$	0.5857
0.15	$y = -18896x + 37.383$	0.4736	$y = -16250x + 32.786$	0.8597
0.20	$y = -15085x + 29.382$	0.1597	$y = -20612x + 39.954$	0.9167
0.25	$y = -20470x + 38.34$	0.4498	$y = -21978x + 41.608$	0.9512
0.30	$y = -26358x + 48.023$	0.6425	$y = -23597x + 43.794$	0.9927
0.35	$y = -26779x + 48.102$	0.7085	$y = -26009x + 47.396$	0.9954
0.40	$y = -30399x + 53.631$	0.7268	$y = -28940x + 51.795$	0.9997
0.45	$y = -31706x + 55.122$	0.6529	$y = -30631x + 54.073$	1
0.50	$y = -32047x + 54.926$	0.4515	$y = -33051x + 57.565$	0.9987
0.55	$y = -20495x + 35.257$	0.1066	$y = -35739x + 61.412$	0.9999
0.60	$y = 46484x - 71.336$	0.5202	$y = -41694x + 70.344$	0.9855
0.65	$y = 19828x - 28.765$	0.9586	$y = -77339x + 125.88$	0.671
0.70	$y = 9436.5x - 12.611$	0.9436	$y = 35345x - 53.41$	0.6697
0.75	$y = 8533.7x - 10.682$	0.8737	$y = 10610x - 14.785$	0.6202
0.80	$y = 4946.5x - 5.7671$	0.5059	$y = 8373.8x - 10.845$	0.5856
0.85	$y = -2531.3x + 2.603$	0.1736	$y = 8250x - 10.043$	0.5681
0.90	$y = -6021.1x + 5.7455$	0.5034	$y = 2969.2x - 3.6046$	0.1338
0.95	$y = -8954x + 8.0513$	0.7712	$y = 5554.4x - 5.4853$	0.0991
0.99	$y = -20999x + 17.512$	0.8667	$y = 46410x - 38.037$	0.4102
1.00	$y = 415533x - 332.66$	0.7987	$y = 50990x - 40.897$	0.2253

Where;  $y = \ln(d\alpha/dt)$  and  $x = 1/T$ .

The cutoff value of  $R^2$  for performing further Friedman analysis was 0.8.

× infers the Friedman analysis inadequate for the determination of activation energy.

√ infers the Friedman analysis adequate for determination of activation energy.

0.85, 0.88 and 0.89 at 20, 30 and 40 °C/min, respectively. Broadly, the gaseous evolution signals shifted to higher  $\alpha$ -value indicating towards more thermal stability in SB. In general, gaseous evolution ( $\text{CH}_4$  or  $\text{H}_2$  or both) TG-signals shifted towards higher temperature with an increase in the  $\beta$  in the case of SS, whereas the shifts in SB for secondary charring signals were seen towards a lower temperature with an increase in  $\beta$ . The gaseous evolution ( $\text{CH}_4$  or  $\text{H}_2$  or both) related transitions were very complex.

Due to melting of lignin because of high temperature generated by high pressure during briquetting, the interface between two jointed particles experienced a layer having high lignin content. This layer was a layer of solidified lignin. Gangil (2014d) explained that the various processes like relaxation, melting and solidification in the lignin bioconstituent occurred under the external stresses. The solidification of lignin was the process which decided about the hardening or softening of the lignin (Gangil, 2014a,b,d). In the case of SB, the present article understood that the distinct presence of hemicellulosic TG-signals in SS as compared to SB, and the sharpening of TG signals (near temperature 750 °C) in SB were among the prominent positive thermogravimetric transitions which were beneficial for briquetting.

#### Kinetics using Friedman method

Friedman curves were drawn at all  $\beta$  and Friedman points ( $1/T$ ,  $\ln(d\alpha/dt)$ ) were taken in the complete range of conversion fraction ( $\alpha$ ), at  $\alpha = 0.05, 0.10, 0.15, 0.20, 0.25, 0.30, 0.35, 0.40, 0.45, 0.50, 0.55, 0.60, 0.65, 0.70, 0.75, 0.80, 0.85, 0.90, 0.95$  and 1.00. Friedman kinetic lines are plotted for both bio-materials. Friedman kinetic lines were more scattered and spread, with respect to entire  $1/T$ -spectrum, in the case of SS as compared to SB indicating that the thermal degradation process was relatively difficult in the case of SB (Fig. 4).

The linear fitting equations for Friedman kinetics lines are given in Table 1. By studying the nature of the slope of the Friedman kinetic lines, the acceleration or retardation nature of the thermal degradation process was ascertained. From Table 1, it can be seen that the process was accelerating in nature until an  $\alpha$ -value of 0.65 for SB and later thermal degradation showed retardation (Lu et al., 2009). In SS, the accelerating nature was until  $\alpha$ -value of 0.55. SS showed retarding thermal degradation in  $\alpha$ -span of 0.6–0.8 and thereafter the process again accelerated to finish the degradation process. The initiation of retardation in SB at a higher  $\alpha$ -value as compared to SS was another evidence for thermal stability of SB. Table 2 shows the higher activation energy levels associated with SB. The activation energy values were in line with activation energies given in several publications for components of lignocelluloses (Gangil, 2014a,b,c,d,e, 2015a,b; White et al., 2011; Tsamba

**Table 2**

Activation energy levels of SS and SB at different conversion fractions in the  $\alpha$ -span of 0.05–0.95.

$\alpha$	Activation energy (kJ/mol)	
	Soybean crop residue (SS)	Briquette (SB)
0.05	47	–
0.15	–	135
0.20	–	171
0.25	–	183
0.30	–	196
0.35	–	216
0.40	–	241
0.45	–	255
0.50	–	275
0.55	–	297
0.60	–	347
0.65	165	–
0.70	78	–
0.75	71	–
0.99	175	–

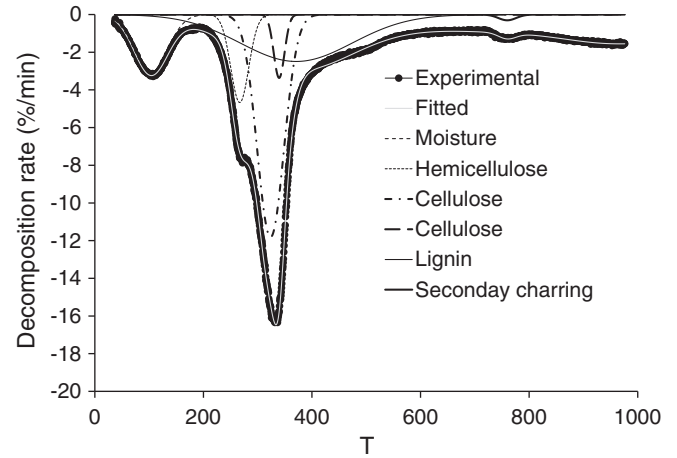


**Fig. 5.** Gaussian deconvolution of DTG (at 30 °C/min) of SS.

et al., 2006). However, the comparison of the SB and SS could not be made using Friedman kinetics because the activation energy levels could not be obtained for both materials at any particular single conversion fraction. This was basically a computational constraint when the conventional kinetics methods are used in the case of lignocellulosic crop residues. This problem was resolved by using deconvolution analysis.

#### Deconvolution analysis of DTG of SS and SB

In order to understand the insights of the thermal degradation of SS and SB, Gaussian deconvolution of DTG of SS and SB was done at each heating rate. Fig. 5 shows a typical deconvolution of SS at a heating rate of 30 °C/min showing the different lumps ascribed to different bioconstituents of SS. The lignin related peak was the flattest showing it as the most difficult intrinsic bioconstituent. Two cellulose related peaks are shown in Fig. 5 related with bi-phasic thermal degradation of cellulose as explained by Gangil, 2014e. Table 3 shows different parameters, amplitude, peak-center and FWHM, of deconvoluted TG-peaks for both materials for DTG taken at 10 °C/min. The full width at half maximum (FWHM) is the measure of sharpness of the peak. The lower FWHM values show sharper peaks and higher values shows flatter peak (Gangil et al., 2008). The flatness of peak is linked with the difficult degradation of the material during thermal degradation. Hemicellulose related peaks showed remarkable higher values of FWHM in the SB indicating for the higher thermal stability. The deconvoluted peaks, related to hemicellulose for SS and SB, are presented in Fig. 6. Lower amplitude and lower T-locations of hemicellulose related deconvoluted TG-signals in SB again indicated for the lesser reactivity in SB (Fig. 6). In relation to cellulose, in the first phase the lesser reactivity was noticed in SB as compared to SS whereas in the second phase, the reactivity increased in SB as compared to SS (Table 4). In the

**Table 3**

Amplitude ( $(d\alpha/dt)_{\max}$ , center ( $T_{\max}$ ) and FWHM of deconvoluted peaks of DTG (at 10 °C/min) of SS and SB.

	SS			SB		
	$(d\alpha/dt)_{\max}$	$T_{\max}$	FWHM	$(d\alpha/dt)_{\max}$	$T_{\max}$	FWHM
Moisture	1.26	68.1	70.8	0.89	107.4	69.3
Hemicellulose	1.41	250.8	36.9	1.17	254.8	66.6
Cellulose	4.27	307.1	59.7	3.20	304.98	58.9
Cellulose	1.59	328.1	30.27	2.69	326.6	24.8
Lignin	1.06	447.6	412.0	0.70	369.4	270.5
Secondary charring	0.43	762.2	153.9	0.11	753.5	28.4

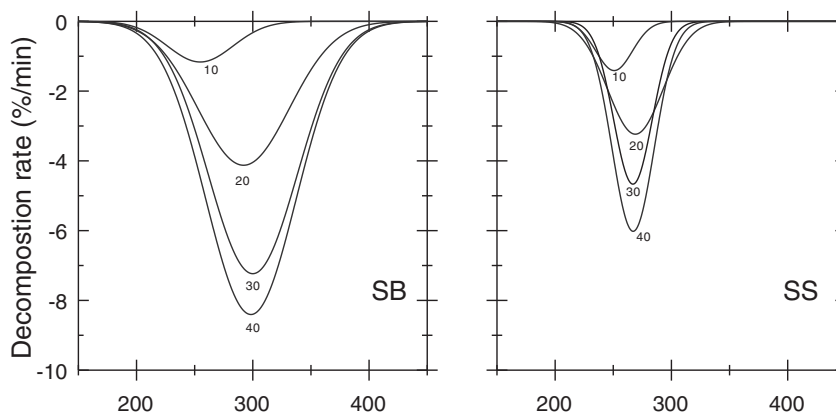


Fig. 6. Transitions of hemicellulose related deconvoluted thermogravimetric signals due to heating rate and also due to briquetting stresses (the numbers 10, 20, 30, and 40 given near the curve, are the heating rates at which the particular DTG was taken).

Table 4

Comparison of amplitude  $(d\alpha/dt)_{\max}$  at all experimented  $\beta$  for different deconvoluted TG-signals for SS and SB.

At $\beta =$	$(d\alpha/dt)_{\max}$							
	10 °C/min		20 °C/min		30 °C/min		40 °C/min	
	SB	SS	SB	SS	SB	SS	SB	SS
Moisture	0.89	1.26	1.71	2.01	2.16	3.05	2.90	3.66
Hemicellulose	1.17	1.41	4.13	3.23	7.236	4.67	8.40	6.02
Cellulose	3.20	4.27	5.20	9.29	6.566	11.82	10.95	18.56
Cellulose	2.69	1.59	6.27	0.90	8.856	3.36	13.16	7.93
Lignin	0.70	1.06	1.23	1.13	1.86	2.49	3.05	3.15
Secondary charring	0.11	0.43	0.27	0.19	0.276	0.30	0.27	0.28

case of lignin, deconvolution analysis showed slightly less reactivity in SB as compared to SS on the basis of comparison of  $(d\alpha/dt)_{\max}$  (Table 4).

## Conclusions

The consolidation of intrinsic biopolymeric components was established in briquettes made from soybean crop residues. In addition to the lignin, the hemicellulose was also found to participate beneficially in the formation of briquette. Activation energies were computed using the integral isoconversional Friedman kinetics method. Deconvolution analysis clearly shows that hemicellulose became less reactive after briquetting.

## Acknowledgements

The author is thankful to the Director (CIAE); PC (AICRP on RES); Head (AEP); and CPI (NAIP-Biomass) for providing facilities and materials. The author acknowledges the help and support received from Mr. PK Das, Mrs. SS Nevase, Mr. K Kujur and Mr. Mohan Verma. The kinetics mentioned in this article is based on TG-results obtained under research activity components of projects 489, 614, 656 and 670 of Central Institute of Agricultural Engineering, Bhopal, India.

## References

Abdullah SS, Yusup S, Ahmad MM, Ramili A, Ismail I. Thermogravimetry study on pyrolysis of various lignocellulosic biomass for potential hydrogen generation. *Int J Chem Biol Eng* 2010;3:137–41.

Burhenne L, Messmer J, Aicher T, Laborie M. The effect of the biomass components lignin, cellulose and hemicellulose on TGA and fixed bed pyrolysis. *J Anal Appl Pyrolysis* 2013;101:177–84.

Caballero JA, Conesa JA, Front R, Marcilla A. Pyrolysis kinetics of almond shells and olive stones considering their organic fractions. *J Anal Appl Pyrolysis* 1997;42:159–75.

Chen W, Kuo P. Isothermal torrefaction kinetics of hemicellulose, cellulose, lignin and xylan using thermogravimetric analysis. *Energy* 2011;36:6451–60.

Chen L, Xing L, Han L. Renewable energy from agro-residues in China: solid biofuels and biomass briquetting technology. *Renew Sustain Energy Rev* 2009;13:2689–95.

Damartzis T, Vamvuka D, Sfakiotakis S, Zabaniotou A. Thermal degradation studies and kinetic modeling of cardoon (*Cynara cardunculus*) pyrolysis using thermogravimetric analysis (TGA). *Bioresour Technol* 2011;102:6230–8.

Đerčan B, Lukić T, Bubalo-Živković M, Đurđev B, Stojsavljević R, Pantelić M. Possibility of efficient utilization of wood waste as a renewable energy resource in Serbia. *Renew Sustain Energy Rev* 2012;16:1516–27.

Dubey AK, Chandra P, Padhee D, Gangil S. Energy from cotton stalks and other crop residues. *icac.org*; 2009 (Available at [https://www.icac.org/projects/CommonFund/20\\_ucbvp/papers/15\\_chandra.pdf](https://www.icac.org/projects/CommonFund/20_ucbvp/papers/15_chandra.pdf)).

Faravelli T, Frassoldati A, Migliavacca G, Ranzi E. Detailed kinetic modeling of the thermal degradation of lignins. *Biomass Bioenergy* 2010;34:290–301.

Fengmin L, Mingquan Z. Technological parameters of biomass briquetting of macrophytes in Nansi Lake. *Energy Procedia* 2011;5:2449–54.

Gangil S. Beneficial transitions in thermogravimetric signals and activation energy levels due to briquetting of raw pigeon pea stalk. *Fuel* 2014a;128:7–13.

Gangil S. Polymeric consolidation in briquetted biofuel as compared to raw biomaterial: a TG-vision for pigeon pea stalks. *Energy Fuel* 2014b;28:3248–54.

Gangil S. Thermogravimetric evidence for better thermal stability in char produced under unconfined conditions. *Environ Eng Sci* 2014c;31:182–93.

Gangil S. Dominant thermogravimetric signatures of lignin in cashew shell as compared to cashew shell cake. *Bioresour Technol* 2014d;155:15–20.

Gangil S. Distinct splitting of cellulose related signals in cashew shell: a TG-diagnosis. *Cellulose* 2014e;21:2913–24.

Gangil S. Benefits of weakening in thermogravimetric signals of hemicellulose and lignin for producing briquettes from soybean crop residue. *Energy* 2015a;81:729–37.

Gangil S. Superiority of intrinsic biopolymeric constituents in briquettes of lignocellulosic crop residues over wood: a TG-diagnosis. *Renew Energy* 2015b;76:478–83.

Gangil S, Nakamura A, Yamamoto K, Ohashi T, Temmyo J. Fabrication and EL emission of ZnO-based heterojunction light-emitting devices. *J Korean Phys Soc* 2008;53:212–7.

Grover PD, Mishra SK. Biomass briquetting technology and practices. Food and Agriculture Organization (FAO), UN Document, 46, 46; 1996 (Available at: <http://www.fao.org/docrep/006/ad579e/ad579e00.pdf>).

Idris SS, Rahman NA, Ismail K, Alias AB, Rashid ZA, Aris MJ. Investigation on thermochemical behaviour of low rank Malaysian coal, oil palm biomass and their blends during pyrolysis via thermogravimetric analysis (TGA). *Bioresour Technol* 2010;101:4584–92.

Janković B. Kinetic analysis of the nonisothermal decomposition of potassium metabisulfite using the model-fitting and isoconversional (model-free) methods. *Chem Eng J* 2008;139:128–35.

Jeguirim M, Bikai J, Elmayer Y, Limousy L, Njeugna E. Thermal characterization and pyrolysis kinetics of tropical biomass feedstocks for energy recovery. *Energy Sustain Dev* 2014; 23:188–93.

Kalayan N, Morey RV. Factors affecting strength and durability of densified biomass products. *Biomass Bioenergy* 2009;33:337–59.

Ledakowicz S, Stolarek P. Kinetics of biomass thermal decomposition. *Chem Pap* 2002;56: 378–81.

López-González D, Fernandez-Lopez M, Valverde JL, Sanchez-Silva L. Thermogravimetric-mass spectrometric analysis on combustion of lignocellulosic biomass. *Bioresour Technol* 2013;143:562–74.

Lu C, Song W, Lin W. Kinetics of biomass catalytic process. *Biotechnol Adv* 2009;27:583–7.

Mandal KG, Saha KP, Ghosh PK, Hati KM, Bandyopadhyay KK. Bioenergy and economic analysis of soybean-based crop production systems in central India. *Biomass Bioenergy* 2002;23:337–45.

Mythil R, Venkatchalam P. Briquetting of agro residues. *J Sci Ind Res* 2013;72:58–61.

Nevase S, Gangde CN, Gangil S. Biomass energy: renewable energy for power generation. Lambert Academic Publishing; 2012 (ISBN-3659299464).

Nevase SS, Gangde CN, Gangil S, Dubey AK. Studies on characterisation of biomass fuel. *Int J Agric Eng Res* 2013;6:547–51.

Purohit P, Tripathi AK, Kandpal TC. Energetics of coal substitution by briquettes of agricultural residues. *Energy* 2006;31:1321–31.

- Rajkumar D, Venkatachalam P. Physical properties of agro residual briquettes produced from cotton, soybean and pigeon pea stalks. *Int. J. Power Eng. Energy* 2013;4:414–7.
- Sanchez-Silva L, López-González D, Villaseñor J, Sánchez P, Valverde JL. Thermogravimetric–mass spectrometric analysis of lignocellulosic and marine biomass pyrolysis. *Bioresour Technol* 2012;109:163–72.
- Sbirrazzuoli N, Vincent L, Mija A, Guigo N. Integral, differential and advanced isoconversional methods: complex mechanisms and isothermal predicted conversion–time curves. *Chemom Intell Lab Syst* 2009;96:219–26.
- Singh RN, Bhoi PR, Patel SR. Modification of commercial briquetting machine to produce 35 mm diameter briquettes suitable for gasification and combustion. *Renew Energy* 2007;32:474–9.
- Singh RN, Vyas DK, Srivastava NSL, Narra M. SPRERI experience on holistic approach to utilize all parts of *Jatropha curcas* fruit for energy. *Renew Energy* 2008;33:1868–73.
- Slopiecka K, Bartocci P, Fantozzi F. Thermogravimetric analysis and kinetic study of poplar wood pyrolysis. *Appl. Energy* 2012;97:491–7.
- Tripathi AK, Iyer PVR, Kandpal TC. A techno-economic evaluation of biomass briquetting in India. *Biomass Bioenergy* 1998;14:479–88.
- Tsamba AJ, Yang W, Blasiak W. Pyrolysis characteristics and global kinetics of coconut and cashew nut shells. *Fuel Process Technol* 2006;87:523–30.
- Tumuluru JS, Wright CT, Kenney KL, Hess JR. A technical review on biomass processing: densification, preprocessing, modeling and optimization. An ASABE meeting presentation paper number: 1009401; 2010. (Available at: <http://www.inl.gov/technicalpublications/documents/4559449.pdf>).
- Vamvuka D, Kakaras E, Kastanaki E, Grammelis P. Pyrolysis characteristics and kinetics of biomass residuals mixtures with lignite. *Fuel* 2003;82:1949–60.
- Vasile C, Popescu C, Popescu M, Brebu M, Willfor S. Thermal behavior/treatment of some vegetable residues. IV. Thermal decomposition of *Eucalyptus* wood. *Cellul. Chem. Technol.* 2011;45:29–42.
- Vyazovkin S, Sbirrazzuoli N. Isoconversional kinetics analysis of thermally stimulated processes in polymers. *Macromol Rapid Commun* 2006;27:1515–32.
- Wang Q, Zhao W, Liu H, Jia C, Xu H. Reactivity and kinetic analysis of biomass during combustion. *Energy Procedia* 2012;17:869–75.
- White JE, Catallo WJ, Legendre BL. Biomass pyrolysis kinetics: a comparative critical review with relevant agricultural residue case studies. *J Anal Appl Pyrolysis* 2011;91:1–33.